SSRG International Journal of Material Science and Engineering
ISSN: 2394–8884 / https://doi.org/10.14445/23948884/IJMSE-V11I3P103

Volume 11 Issue 3, 11-14, Sep-Dec 2025

Original Article

Engineering of CdSe, CdS, and ZnS Quantum Dots for Narrow Bandgap Devices Using the Effective Mass Approximation

G.C. Ogbu[1], O. K. Okongwu[4], E.N. Nwaru[3], U. D. Chukwuma[5], D. N. Ndubueze[2], S. C. Igbokwe[6], L. U. Uwenwa[7]

[1,2]*Department of Industrial Physics, Enugu State University of Science and Technology.*
[3]*Department of Electrical/Electronics Engineering, Eastern Polytechnic, Rivers State*
[4]*Department of Industrial Mathematics, Enugu State University of Science and Technology.*
[5,6]*Department of Physics, Kingsley Ozumba Mbadiwe University, Ogboko Ideato, Imo State.*
[7]*Department of Electrical/Electronics Engineering, Cross Rivers State University*

Received: 01 October 2025 Revised: 03 November 2025 Accepted: 19 November 2025 Published: 08 December 2025

Abstract - *This work presents a theoretical investigation of the size-dependent bandgap variation in CdSe, CdS, and ZnS Quantum Dots (QDs) using the Effective Mass Approximation (EMA) within the framework of the Brus equation. The model accounts for the intrinsic bulk bandgap, the quantum confinement contribution arising from carrier spatial restriction, and the Coulombic interaction between electrons and holes to predict bandgap energies across a radius range of 1–10 nm. Material-specific parameters, such as effective electron and hole masses and dielectric constants, were extracted from established experimental data to ensure accurate estimation. The analysis shows that the effective bandgap energy increases markedly as the QD radius decreases, confirming the inverse relationship between size and bandgap. Among the examined materials, CdSe QDs demonstrate the greatest potential for narrow bandgap engineering, with their bandgap tunable from the bulk value of ~1.74 eV into the near-infrared regime at larger radii. By contrast, CdS and ZnS QDs, with higher intrinsic bandgaps (2.42 eV and 3.68 eV, respectively), exhibit stronger confinement-induced shifts and are therefore more suitable for ultraviolet and visible-light applications. Nevertheless, when employed in core–shell heterostructures such as CdSe/ZnS or CdSe/CdS, CdS and ZnS provide critical advantages in surface passivation, stability enhancement, and suppression of nonradiative recombination, while enabling CdSe cores to preserve their narrow bandgap functionality. Overall, this study reinforces the effectiveness of EMA in predicting quantum confinement effects in semiconductor nanocrystals and provides valuable theoretical guidance for the experimental synthesis and integration of CdSe-, CdS-, and ZnS-based QDs into next-generation optoelectronic and photonic devices.*

Keywords - *Quantum Dots, Effective Mass Approximation (EMA), Brus Equation, CdSe, CdS, ZnS, Bandgap Engineering, Narrow Bandgap Devices, Optoelectronics.*

1. Introduction

Semiconductor nanostructures have emerged as transformative materials in modern optoelectronics owing to their unique electronic and optical properties, which differ markedly from those of their bulk counterparts. Among these, Quantum Dots (QDs) are particularly significant. As zero-dimensional systems, QDs confine both electrons and holes in all three spatial dimensions, resulting in discrete, atom-like energy states and strongly size-dependent optical and electronic behaviors [1,2]. This quantum confinement effect enables precise tuning of bandgap energies through control of QD radius, thereby supporting applications ranging from visible light-emitting diodes to infrared photodetectors [3].

The theoretical basis for size-dependent bandgap modulation in QDs was first established by Brus, who formulated what is now known as the Brus equation, derived from the Effective Mass Approximation (EMA) [4]. In this framework, charge carriers are modeled as free particles with effective masses confined within a spherical potential well. The equation incorporates contributions from the bulk bandgap, confinement-induced kinetic energy, and Coulombic electron–hole interactions. Although simplified, EMA provides a robust first-order description of bandgap variations in II–VI and III–V semiconductor nanocrystals [5]. Within the diverse family of QDs, cadmium chalcogenides, notably cadmium selenide (CdSe), cadmium sulfide (CdS), and zinc sulfide (ZnS), have been extensively studied due to their well-

characterized bulk band structures, tunable excitonic transitions, and versatile synthetic methods [6]. Bulk CdSe has a direct bandgap of ~1.74 eV, CdS ~2.42 eV, and ZnS ~3.68 eV. When the particle radius approaches or falls below the exciton Bohr radius, these values can shift significantly, allowing precise bandgap engineering across the visible to Near-Infrared (NIR) spectrum [7].

For narrow bandgap device applications, including NIR photodetectors, Quantum Dot Infrared Photodetectors (QDIPs), third-generation photovoltaics, and infrared light-emitting devices, the ability to reduce and finely tune the bandgap is critical [8]. CdSe QDs, owing to their relatively small intrinsic bandgap, can be tuned efficiently into the NIR regime, making them strong candidates for such applications. In contrast, CdS and ZnS, with larger bandgaps, are more suitable for ultraviolet and high-energy visible emission. However, their integration in core–shell heterostructures (e.g., CdSe/ZnS or CdSe/CdS) plays a crucial role in enhancing photostability, suppressing nonradiative recombination, and improving quantum yield, thereby extending the performance of CdSe-based narrow bandgap devices [9,10]. Consequently, a systematic investigation of bandgap engineering in CdSe, CdS, and ZnS QDs using EMA provides a theoretical framework for tailoring their optical responses to diverse optoelectronic technologies. The present study employs the Brus equation to analyze the dependence of bandgap energy on QD radius and elucidates the comparative advantages of these three materials for narrow bandgap device applications.

2. Literature Review

2.1. Effective Mass Approximation (EMA)

The Effective Mass Approximation (EMA) simplifies the motion of electrons and holes inside a Quantum Dot (QD) by treating them as free particles, but with effective masses $m_{e,}^{*}$ and m_h^*, that accounts for the influence of the crystal lattice. In a spherical quantum dot of radius R, the total bandgap can be expressed as the sum of three contributions:

$$E_g(R) = E_{bulk} + E_{conf}(R) - E_{coul}(R) \quad (1)$$

2.1.1. Bulk Bandgap Energy (E_{bulk})

This represents the intrinsic bandgap of the bulk semiconductor:

2.1.2. Confinement Energy ($E_{conf}(R)$)

This represents the increase in bandgap due to the spatial confinement of charge carriers:

$$E_{conf}(R) = \frac{\hbar^2\pi^2}{2R^2}\left(\frac{1}{m_e^*} + \frac{1}{m_h^*}\right) \quad (2)$$

As the radius R decreases, the confinement energy increases significantly, leading to a blue shift in absorption and emission spectra.

2.1.3. Coulomb Interaction Energy ($\boldsymbol{E_{coul}(R)}$)

This accounts for the attractive interaction between the electron and hole:

$$E_{coul}(R) = \frac{1.8e^2}{4\pi\varepsilon_o\varepsilon_r R} \quad (3)$$

Although this term reduces the bandgap, it is generally smaller than the confinement energy, particularly for very small radii.

2.2. Brus Equation

By combining the three contributions above, the size-dependent bandgap of a quantum dot can be expressed using the Brus Equation (Brus, 1984):

$$E_g(R) = E_{bulk} + \frac{\hbar^2\pi^2}{2R^2}\left(\frac{1}{m_e^*} + \frac{1}{m_h^*}\right) - \frac{1.8e^2}{4\pi\varepsilon_o\varepsilon_r R} \quad (4)$$

This equation provides a practical means to estimate the optical bandgap of QDs of a given radius, capturing the effects of both confinement and Coulomb interaction.

1. Materials and Methods

This study adopts a theoretical approach, employing Effective Mass Approximation (EMA)based calculations to evaluate the bandgap energies of CdSe, CdS, and ZnS quantum dots across radii ranging from 1 to 10 nm. The computed results are plotted for each material to illustrate the effects of quantum confinement, enabling a clear visualization of bandgap tunability with size reduction. The analysis further identifies the optimal radius ranges that support narrow-bandgap device applications. All material-specific parameters, including effective masses and dielectric constants, were sourced from established literature and are summarized in Table 1.

Table 1. Exciton Bohr Radius and Related Parameters

Material	E_g, **bulk** (eV)	$\frac{m_e^*}{m_0}$	$\frac{m_h^*}{m_0}$	ε_r	Exciton Bohr Radius (nm)
CdSe	1.74	0.13	0.45	9.5	~5.6
CdS	2.42	0.21	0.50	5.7	~2.9
ZnS	3.70	0.28	0.59	8.1	~2.5

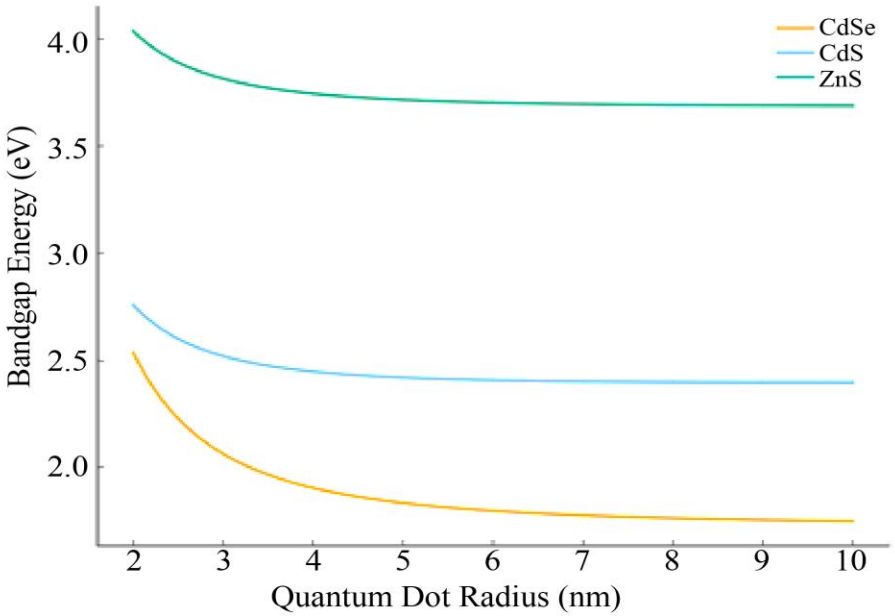

Fig. 1 Size-Dependent Bandgap of CdSe, CdS, and ZnS Quantum Dots (EMA Model)

2. Results and Discussion

The calculated bandgap energies of CdSe, CdS, and ZnS quantum dots as a function of radius (2–10 nm) are presented in Figure 1. The results demonstrate a pronounced size-dependent variation, providing clear evidence of quantum confinement, which is fundamental to their suitability for narrow bandgap device applications. As expected, the bandgap energy increases with decreasing particle radius, and the magnitude of this shift is strongly influenced by the intrinsic exciton Bohr radius of each material.

CdSe possesses the lowest bulk bandgap (1.74 eV) among the three materials and the largest exciton Bohr radius (~5.6 nm), which gives it the highest degree of size-dependent tunability across the visible and Near-Infrared (NIR) spectrum. At larger radii (~7–10 nm), its bandgap remains close to the bulk value (1.7–1.8 eV), corresponding to red/NIR absorption and emission. This makes CdSe QDs particularly attractive for narrow-bandgap photodetectors employed in optical communication, night-vision systems, and biomedical imaging. At smaller radii (~3–5 nm), the bandgap increases to ~2.1–2.3 eV, enabling efficient optical activity in the green–yellow range.

Such tunability is especially advantageous in multi-junction solar cells, where CdSe QDs can be engineered to match intermediate sub-bandgaps for enhanced photon harvesting. Moreover, CdSe's strong radius-dependent behavior supports applications in QD-LEDs and low-threshold lasers, where precise bandgap control facilitates narrowband visible emission. Overall, CdSe emerges as the primary candidate for narrow-bandgap devices, as its bandgap can be tuned continuously from the NIR into the visible region.

CdS, in contrast, has a wider bulk bandgap (2.42 eV) and a smaller Bohr radius (~2.9 nm), which leads to more moderate bandgap tunability. At larger radii (>6 nm), CdS QDs retain bandgaps near their bulk value (2.4–2.5 eV), corresponding to absorption in the visible-blue range. When reduced to ~2–3 nm, the bandgap increases to ~3.0–3.1 eV, extending further into the blue/UV region. While this limits CdS as a primary absorber for narrow-bandgap applications, it plays critical supporting roles. For instance, in QD-sensitized solar cells (QDSSCs), CdS can act as a sensitizer by efficiently injecting electrons into TiO_2 scaffolds while pairing with CdSe to broaden spectral absorption. Similarly, in heterojunction devices (e.g., CdSe/CdS), CdS serves as a buffer or window layer that enhances charge transfer while CdSe provides the NIR absorption. Thus, CdS contributes to device engineering not as a narrow-bandgap absorber itself, but as a complementary material that improves carrier dynamics and interfacial performance.

ZnS, with the largest bulk bandgap (3.7 eV) and the smallest Bohr radius (~2.5 nm), exhibits the least bandgap tunability. At very small radii, its bandgap exceeds 4.5 eV, restricting its spectral response to the ultraviolet region. Consequently, ZnS QDs are unsuitable as absorbers in narrow-bandgap devices. Nonetheless, ZnS plays an indispensable role as a shell material in core–shell architectures such as CdSe/ZnS and CdS/ZnS. Its wide bandgap confines charge carriers within the CdSe or CdS core, effectively suppressing nonradiative recombination and significantly enhancing photoluminescence quantum yield. Additionally, ZnS provides robust chemical stability, protecting narrow-bandgap cores from photo-oxidation and environmental degradation, factors critical for long-term device performance. Therefore, while ZnS cannot directly

function as a narrow-bandgap absorber, it indirectly supports such applications by enhancing the efficiency, stability, and durability of CdSe- and CdS-based QDs.

3. Conclusion

This study demonstrates the bandgap engineering of CdSe, CdS, and ZnS Quantum Dots (QDs) within the Effective Mass Approximation (EMA) framework. The results confirm a strong size-dependent variation in bandgap energy, underscoring the tunability that is critical for narrow-bandgap device design. Among the three materials, CdSe QDs exhibit the greatest versatility, with their bandgap adjustable across the visible–NIR range, making them the most suitable candidates for narrow-bandgap applications. CdS QDs, while less tunable, function effectively as complementary sensitizers or buffer layers, enhancing charge transfer and modestly extending absorption in device architectures. ZnS QDs, though unsuitable as absorbers, play a vital role as passivating shells that stabilize CdSe and CdS cores, suppress nonradiative recombination, and improve long-term performance. Collectively, these findings provide theoretical guidelines for experimental synthesis and integration of cadmium chalcogenide QDs, supporting their deployment in infrared detectors, nanophotonic devices, and advanced photovoltaic systems.

References

[1] A.P. Alivisatos, "Perspectives on the Physical Chemistry of Semiconductor Nanocrystals," *The Journal of Physical Chemistry*, vol. 100, no. 31, pp. 13226-13239, 1996. [CrossRef] [Google Scholar] [Publisher Link]

[2] A.L. Efros, and M. Rosen, "The Electronic Structure of Semiconductor Nanocrystals," *Annual Review of Materials Science*, vol. 30, pp. 475-521, 2000. [CrossRef] [Google Scholar] [Publisher Link]

[3] Victor I. Klimov, *Semiconductor and Metal Nanocrystals: Synthesis and Electronic and Optical Properties*, CRC Press, 2000. [Google Scholar] [Publisher Link]

[4] L.E. Brus, "Electron–Electron and Electron–Hole Interactions in Small Semiconductor Crystallites: The Size Dependence of the Lowest Excited Electronic State," *The Journal of Chemical Physics*, vol. 80, no. 9, pp. 4403-4409, 1984. [CrossRef] [Google Scholar] [Publisher Link]

[5] Yosuke Kayanuma, "Quantum-Size Effects of Interacting Electrons and Holes in Semiconductor Microcrystals with Spherical Shape," *Physical Review B*, vol. 38, no. 14, pp. 9797-9805, 1988. [CrossRef] [Google Scholar] [Publisher Link]

[6] C.B. Murray, D.J. Norris, and M.G. Bawendi, "Synthesis and Characterization of Nearly Monodisperse CdE (E = S, Se, Te) Semiconductor Nanocrystallites," *Journal of the American Chemical Society*, vol. 115, no. 19, pp. 8706-8715, 1993. [CrossRef] [Google Scholar] [Publisher Link]

[7] Debasis Bera et al., "Quantum Dots and Their Multimodal Applications: A Review," *Materials*, vol. 3, no. 4, pp. 2260-2345, 2010. [CrossRef] [Google Scholar] [Publisher Link]

[8] P. Martyniuk, and A. Rogalski, "Quantum-Dot Infrared Photodetectors: Status and Outlook," *Progress in Quantum Electronics*, vol. 32, no. 3-4, pp. 89-120, 2008. [CrossRef] [Google Scholar] [Publisher Link]

[9] B.O. Dabbousi et al., "(CdSe)ZnS Core–Shell Quantum Dots: Synthesis and Characterization of a Size Series of Highly Luminescent Nanocrystallites," *The Journal of Physical Chemistry B*, vol. 101, no. 46, pp. 9463-9475, 1997. [CrossRef] [Google Scholar] [Publisher Link]

[10] AL. Rogach, DV. Talapin, and H. Weller, *Semiconductor Nanoparticles*, Colloids and Colloid Assemblies: Synthesis, Modification, Organization and Utilization of Colloid Particles, Wiley, pp. 52-91, 2003. [Google Scholar] [Publisher Link]